Do short-time fluctuations predict the long-time dynamic heterogeneity in a supercooled liquid?

J. A. Rodriguez Fris, L. M. Alarcón, and G. A. Appignanesi
Fisicoquímica, Departamento de Química, Universidad Nacional del Sur, Avenida Alem 1253, 8000 Bahía Blanca, Argentina
(Received 7 March 2007; revised manuscript received 26 May 2007; published 2 July 2007)

Recent investigations have demonstrated that the short-time fluctuations in a supercooled liquid can be used as predictors of the long-time dynamic propensity (that is, the regions of the sample with enhanced tendency to be mobile within time scales on the order of the α-relaxation time). This could mean that the long-time dynamics (the actual mobility of the particles at such long times) would be implicit in the short-time dynamics or else, that the long-time dynamic propensity [as defined in A. Widmer-Cooper and P. Harrowell, Phys. Rev. Lett. **96**, 185701 (2006)], while providing a measure of the degree of jamming of the local structure, would only be sensitive to the short time behavior. The first scenario is in clear disagreement with our recent finding that the influence of the local structure on dynamics (as determined by the propensity for motion) is only local in time, fading out at times close to the metabasin lifetime, much before the α-relaxation time. Thus, in this work we show that the short-time fluctuations in supercooled liquids do in fact represent precursors to the dynamics at intermediate times commensurate with the metabasin lifetime (being thus able to predict the regions of the sample that will present high propensity for motion at such stage) but that the dynamical behavior at later times of the α relaxation is unpredictable, in agreement with a metabasin random walk scenario.

DOI: 10.1103/PhysRevE.76.011502 PACS number(s): 64.70.Pf, 61.20.Ja, 61.20.Lc

I. INTRODUCTION

The relaxation of glassy liquids has been demonstrated to be dynamically heterogeneous and to proceed by means of the development of slowly relaxing domains that grow both in size and time scale as temperature is lowered in the supercooled regime [1–10]. Thus, at each time dynamics vary considerably from one point of the sample to another, a fact that suggests the intuitively plausible picture of the existence of regions with different degree of structural "jamming" [8,10]. However, despite its paramount importance and the amount of work devoted to it [1], the determination of a causal link between structure and dynamics in supercooled liquids remains as an open issue. Within this context, a beautiful recent work [8] has demonstrated that certain aspect of dynamical heterogeneity indeed depends on structure: while dynamical heterogeneities and particle motions are not reproducible, the spatial variation of the propensity for motion (the tendency of the particles to be mobile) is completely determined by the initial structural configuration, thus establishing a link between structure and dynamics. More recently, some of these authors published a paper [11] where they showed that while neither the potential energy nor the free-volume of the structure of a two-dimensional (2D) glass-former is related to propensity, the short-time fluctuations (as measured by the Debye Waller factors) constitute precursors of the long-time propensity: They found that the regions of enhanced short-time motion were coincident with the regions of high propensity calculated at $1.5\tau_e$ [with τ_e being the α-relaxation time estimated as the time when the incoherent intermediate scattering function $F_s(q,t)$, measured at the wave vector q of the first peak in the structure factor, has decayed to $1/e$] a time scale about two orders of magnitude larger. This is a nice result which could emerge from the occurrence of two distinct dynamical scenarios.

(1) The particles and regions that are mobile at short times remain dynamically active at long times ($t=1.5\tau_e$) so that the long-time motions of the particles would be implicit in the short-time dynamics.

(2) The heterogeneous nature of the propensity at long times is due largely to the behavior at short times and there is little additional correlation arising from the later times (with propensity representing only a measure of the short-time motions irrespective of the time scale chosen to calculate it). This last case would imply that the particles and regions that are mobile at $t=1.5\tau_e$ would be completely different from the ones that were active at short times. Thus, while the short-time fluctuations accurately predict the long-time propensity, they cannot predict the long-time dynamics (the mobile regions at long times).

Only the second possibility is consistent with our recent finding [10] on binary Lennard-Jones systems (by means of an extension of the propensity concept) that the influence of structure on dynamics fades out quickly after the metabasin (MB) lifetime, a time scale much shorter than the α-relaxation time (a MB is a finite region of configuration space including many different local minima which confines the system for a fraction of the structural relaxation time, while the crossing between MBs is a rapid event produced by the fast diffusional movement of a significant group of dynamically correlated particles that form a relatively compact cluster, called "democratic" cluster or d cluster, which represents a relevant step in the α relaxation [9,10]). This is so since the trajectory can reach many different MBs from a given one and the long-time dynamics represents a random walk on MBs [7,10,12], a scenario which could hardly be reconciled with the results of Ref. [11]. On the contrary, the first case (completely compatible with the results of Ref. [11]) is in obvious disagreement with Ref. [10]. Thus, in the present work we aim at addressing the question of whether the dynamical behavior at later times is in fact implicit in the short-time fluctuations of the system and, if so, which is the time scale over which the short-time dynamics can be used to predict the spatial distribution of dynamical heterogene-

ities. In this regard, our work shall demonstrate that while the short-time relaxation of the system can be used to accurately predict the behavior at intermediate times commensurate with the MB lifetime, the long time dynamics is indeed not predictable. By so doing, we shall furnish a picture for the emergence and relaxation of structurally "unjammed" regions in the system.

II. RESULTS AND DISCUSSION

We performed a series of molecular dynamics (MD) simulations within the NVE ensemble for a paradigm model of fragile glass former: the binary Lennard-Jones system consisting of a 3D mixture of 80% A and 20% B particles, the size of the A particles being 47% larger than the B ones [5,9,13]. We shall show results from systems at temperature $T=0.5$, density of 1.2 and 150 particles [9]. We have chosen this system size to avoid the interference of results from many different subsystems (MBs) while being free of finite size effects, as shown in Ref. [9]. At low temperatures (close to and above the mode coupling temperature, $T_c=0.435$) this system presents dynamical heterogeneities [5,9]: a small number of particles move cooperatively a distance that is comparable to the inter-particle distance. These "fast-moving" (or "mobile") particles are not homogeneously distributed throughout the sample but are arranged in clusters usually made of stringlike groups of particles [5,9]. The dynamics is most heterogeneous at a time t^* defined by the maximum in the non-Gaussian parameter $\alpha_2(t)$, $\alpha_2(t)=\frac{3\langle r^4(t)\rangle}{5\langle r^2(t)\rangle^2}-1$, which measures the deviation of the self-part of the van Hove function $4\pi r^2 G_s(r,t)$, the probability at a given time t of finding a particle at distance r from its initial position at $t=0$, from a Brownian behavior [5]. This quantity is located at the end of the β beginning of the α relaxation (the crossover from the caging to the diffusive regime in the mean squared displacement plot) and constitutes the characteristic time for dynamical heterogeneities (in this case $t^*=400$, [9]). Additionally, t^* depends strongly on temperature and grows quickly as we move towards T_c [5]. However, not all the mobile particles within a t^* time span contribute decisively to the α relaxation, as we have recently demonstrated [9]. Instead, the α relaxation is driven by a series of a few MB transitions which are triggered by the occurrence of collective events characterized by large compact clusters of medium-range mobile particles called democratic motions [9]. Additionally, the mean residence time in a MB τ_{MB} has been estimated to be close to t^* [9,10]. These events initially discovered in binary Lennard-Jones systems [9] are also being verified in other glassy systems such as supercooled water [14]. Recently, a very nice mixed computational-experimental work [15] provided experimental verification for these collective movements and MB transitions. In such work [15] our methods [9] were used to explain the physical origin of the hopping behavior observed in single molecule fluorescence measurements in glassy polymers, thus gaining a hitherto non available experimental resolution.

To calculate the propensity for motion we use the isoconfigurational (IC) method introduced in Ref. [8]. In it one performs a series of equal length MD runs (trajectories) from the same initial configuration, that is, always the same structure (the same particle positions) but each one with different initial particle momenta chosen at random from the appropriate Boltzmann distribution (that is, one builds an IC ensemble). For times when the system is dynamically heterogeneous, each run or trajectory presents mobile particles arranged in open (usually string-like) clusters. However, the mobile particles and corresponding clusters differ from run to run since the mobility of the particles in a single run is not determined by the initial configuration [8]. Propensity of a particle for motion in the initial configuration (its tendency to be mobile) for a fixed time interval of length t has been defined as [8,10] $\langle \Delta \mathbf{r}_i^2 \rangle_{\mathrm{IC}}$, where $\langle \cdots \rangle_{\mathrm{IC}}$ indicates an average over the IC and $\Delta \mathbf{r}_i^2=[\mathbf{r}_i(t=t)-\mathbf{r}_i(t=0)]^2$ is the squared displacement of particle i in such time interval. At low temperatures propensities are not uniform throughout the sample and high propensity particles are confined to certain (relatively compact) regions [8,10]. Thus, while particle mobility is not reproducible from run to run, the spatial variation in the propensity is completely determined by the initial configuration, reflecting the influence of structure on dynamics [8,10].

In Ref. [10] we defined a time-dependent propensity for a given time interval (in that case of length t^*). That is, one calculates propensities for time interval $[t,t+\delta]$, which gives the tendency of the particles to be mobile within such time interval (in our previous work we used $\delta=t^*$ [10]). In other words, one starts many IC runs at $t=0$ but calculates propensities as $\langle \Delta \mathbf{r}_i^2(t,\delta)\rangle_{\mathrm{IC}}=\langle [\mathbf{r}_i(t+\delta)-\mathbf{r}_i(t)]^2\rangle_{\mathrm{IC}}$. We recall that this definition of the propensity implies that while all the trajectories have been started from the same initial configuration, here we measure the tendency of the particles to be mobile *within* the different time intervals indicated. With this method we found that particle propensities clearly become uniform very quickly (they quench and fluctuate smoothly around the mean value) for times slightly greater than $t=t^*$, much before the time of the α relaxation (τ_α is about an order of magnitude greater than t^* [10]). Hence, a main conclusion emerged [10]: The influence of structure on dynamics is only local in time in which concerns the propensity for motion, being thus influential for the β but not for the α relaxation. Thus, the propensity represents a measure of the degree of jamming (the particles and regions with different tendency to mobility) of the structure at time t, the beginning of the corresponding time interval [10,16].

We now first calculate propensity for different times $\langle \Delta \mathbf{r}_i^2(0,\delta)\rangle_{\mathrm{IC}}$, with $\delta=0.01t^*$, $0.1t^*$, t^*, and $4t^*$, that is, $\delta=4$, 40, 400, and 1600, as shown in Fig. 1. We made such a choice in order to compare our results with the ones of Ref. [11]. This is so since in Ref. [11] a time interval of length $1.5\tau_e$ was used. In our system, such time corresponds to $4t^*=1600$ in reduced units [in other works we have estimated τ_α when $F_s(q,t)$ has decayed to 10%, which here occurs at $t=4000$]. In such a figure we show the individual particle propensities for the 120 A particles. We can see that propensity is heterogeneously distributed with some particles displaying values much larger than the mean value. We can also corroborate the results of Ref. [11] since the short- and long-time behaviors are similar in which concerns the propensity

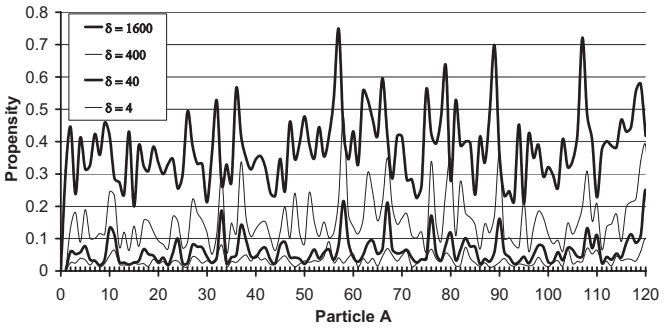

FIG. 1. Propensity for the 120 A particles for δ=1600, 400, 40, and 4 (from the curve on the top to the one at the bottom, respectively) in reduced time units.

distribution, which means that the short-time behavior predicts the long-time propensity. However, we note here that this does not mean that the long-time dynamics is predicted, that is, the particles or regions that will be mobile at the long times commensurate with the structural relaxation time. Widmer-Cooper and Harrowell [11] do not make any consideration regarding this point and choose to calculate the propensity at a time two orders of magnitude larger ($t=1.5\tau_e$) than that used for evaluation of the short-time motions, while, as we shall see later on, any time in between would produce equivalent results.

To test if the short-time behavior affects the long-time dynamics we now calculate the time-dependent propensity [10] $\langle \Delta \mathbf{r}_i^2(t,\delta)\rangle_{\mathrm{IC}}=\langle[\mathbf{r}_i(t+\delta)-\mathbf{r}_i(t)]^2\rangle_{\mathrm{IC}}$, with δ=40 and for two different independent IC ensembles (or initial structures) each of 1200 trajectories at T=0.5. This low value of δ means that one is sampling the very short-time motions (in fact, the tendency to be mobile within the IC) of the particles precisely at time t (within time intervals $[t,t+\delta]$, 1% of the α-relaxation time). Figure 2 shows that for the two cases the ratio of the dispersion to the mean value ($\sigma/\langle P\rangle$, with $\langle P\rangle$ denoting the mean propensity value) falls quickly and the propensity loses its heterogeneous nature much before the long time scales used in Ref. [11]. In such figure we also

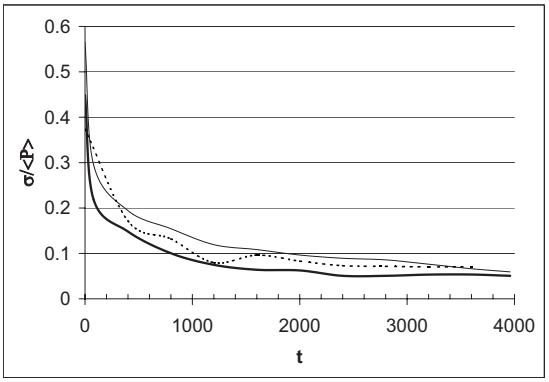

FIG. 2. $\sigma/\langle P\rangle$ as a function of reduced time t for two different IC ensembles at the same temperature. The thick solid line corresponds to the IC of Fig. 1 (and to all the following figures in this work) and δ=40. The dashed line is the same curve calculated with δ=400 while the thin solid line corresponds to the curve for another ensemble calculated with δ=40.

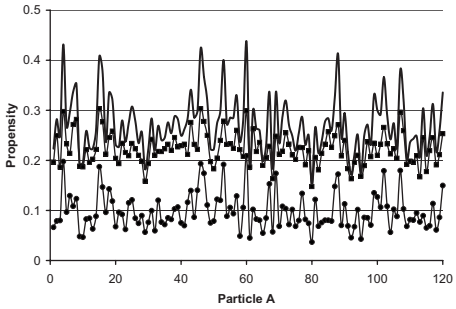

FIG. 3. $\langle \Delta \mathbf{r}_i^2(0,400)\rangle_{\mathrm{IC}}$ (dots), $\langle \Delta \mathbf{r}_i^2(400,1600)\rangle_{\mathrm{IC}}$ (squares), and $\langle \Delta \mathbf{r}_i^2(0,1600)\rangle_{\mathrm{IC}}$ (solid line, no symbols) for the different A particles.

included a curve for a larger value of δ=400 (but still much lower than the α-relaxation time) which yields results which are consistent with the ones that arise with the lower value of δ.

In turn, Fig. 3 shows $\langle \Delta \mathbf{r}_i^2(0,400)\rangle_{\mathrm{IC}}$ (dots), $\langle \Delta \mathbf{r}_i^2(400,1600)\rangle_{\mathrm{IC}}$ (squares), and $\langle \Delta \mathbf{r}_i^2(0,1600)\rangle_{\mathrm{IC}}$ (solid line) for the different A particles. From direct inspection of these curves we can learn that most of the heterogeneity in the propensity for the complete large time span [0, 1600] comes from the behavior at the shortest time interval [0, 400], while the rest of the time (the time interval [400,1600]) basically adds to the mean propensity but does not contribute significantly to the heterogeneity. For comparison, the value of $\sigma/\langle P\rangle$ for the time interval [0,400] is 0.373 while for the time interval [400,1600] is only 0.141 (for the whole time interval, [0,1600], it amounts to 0.272). That is, the heterogeneity in the propensity at $1.5\tau_\alpha$ is largely laid down at short times, with little additional correlation arising from the rest of the time.

To make this point more evident, in Fig. 4(a) we show $\langle \Delta \mathbf{r}_i^2(0,400)\rangle_{\mathrm{IC}}$ (solid line), $\langle \Delta \mathbf{r}_i^2(400,800)\rangle_{\mathrm{IC}}$ (dots), and $\langle \Delta \mathbf{r}_i^2(1600,2000)\rangle_{\mathrm{IC}}$ (squares) for the different A particles (we note that the mean propensity value is basically the same for the three cases). We can clearly see from this figure that only for the propensity calculated at short times (time interval [0,400]) this quantity is broadly distributed among the A particles, with some particles displaying propensities much larger than the mean value. For the other two cases the propensity is much more narrowly distributed around the mean value. In Fig. 4(b) we show results for smaller time intervals, that is, $\langle \Delta \mathbf{r}_i^2(0,40)\rangle_{\mathrm{IC}}$ (solid line), $\langle \Delta \mathbf{r}_i^2(400,440)\rangle_{\mathrm{IC}}$ (dots), and $\langle \Delta \mathbf{r}_i^2(1600,1640)\rangle_{\mathrm{IC}}$ (squares). Again the results show (here even more markedly) that propensity is only heterogeneous at short times.

In order to better state the timescale at which the short-time dynamics can be regarded as a predictor of the spatial structure of dynamical heterogeneity, we divided the $[0,10t^*]$ time span in 10 equal length time intervals and calculated the number of high propensity particles in each of them [we recall that $t=10t^*=4000$ is the time at which $F_s(q,t)$ has decayed to 10% its initial value, and also represents a measure of τ_α]. We considered as particles of high propensity that whose propensity $\langle \Delta \mathbf{r}_i^2(t,t+t^*)\rangle_{\mathrm{IC}}$ (with $t=0,t^*,2t^*,\ldots,9t^*$, that is, $t=0,400,800,\ldots,3600$) was 36,

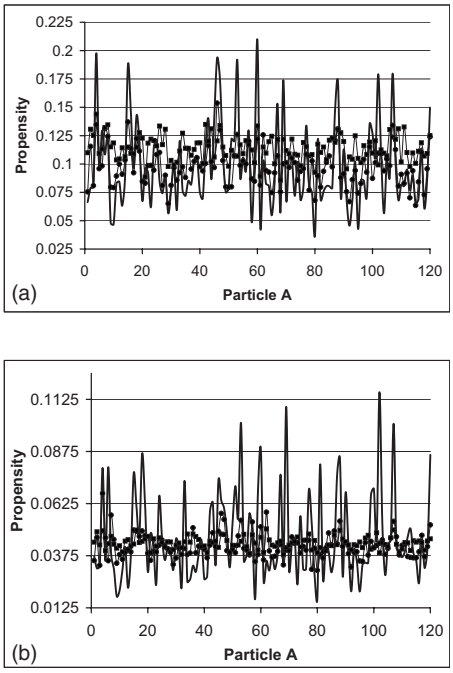

FIG. 4. (a) $\langle \Delta \mathbf{r}_i^2(0,400)\rangle_{\mathrm{IC}}$ (solid line, no symbols), $\langle \Delta \mathbf{r}_i^2(400,800)\rangle_{\mathrm{IC}}$ (dots), and $\langle \Delta \mathbf{r}_i^2(1600,2000)\rangle_{\mathrm{IC}}$ (squares) for the different A particles. (b) Same as in (a) but for smaller time spans, that is, $\langle \Delta \mathbf{r}_i^2(0,40)\rangle_{\mathrm{IC}}$ (solid line, no symbols), $\langle \Delta \mathbf{r}_i^2(400,440)\rangle_{\mathrm{IC}}$ (dots), and $\langle \Delta \mathbf{r}_i^2(1600,1640)\rangle_{\mathrm{IC}}$ (squares).

50, 75, and 100% greater than the corresponding value of $\langle P\rangle$ (we recall that $\langle P\rangle$ is almost invariant for the different time intervals while σ falls abruptly with increasing time). The first value was chosen since $\langle P\rangle + 36\% \langle P\rangle = \langle P\rangle + 3\sigma$ for the entire time span $[0,t^*]$. The first interval, $[0t^*]$ (that is [0,400]), exhibits 16, 11, 8, and 2% of its A particles with propensity 36, 50, 75 and 100%, greater than $\langle P\rangle$, respectively. The second time interval, $[t^*,2t^*]$ (that is [400,800]), only presents 3, 1, 0, and 0%, respectively. None of the other eight time intervals present high propensity particles in the ranges considered. Thus, these results indicate that no significant high propensity regions can be found for times beyond t^*.

Figure 5 displays the three dimensional arrangement of the high propensity particles for selected time intervals. Again we select high propensity particles as that whose propensity is 36, 50, 75, and 100% greater than the value of $\langle P\rangle$ for the corresponding time interval. We show results for time intervals $[0,0.1t^*]$, $[0,t^*]$, and $[0,4t^*]$. We also show the case for $[0,10t^*]$, where we plot the 10% of the A particles with higher propensity (corresponding to $\langle \Delta \mathbf{r}_i^2(0,10t^*)\rangle_{\mathrm{IC}}\rangle$ ($\langle P\rangle + 1.4\sigma$), with $\langle P\rangle$ and σ being the mean propensity value and the dispersion for such time interval). We can clearly see that the high propensity regions are quite similar in all cases. In particular, such regions for $[0,0.1t^*]$ and $[0,t^*]$ look very much alike. We recall that from the ten t^*-length consecutive time intervals in which we divided the time span $[0,10t^*]$, only the one plotted ($[0,t^*]$) exhibits a significant high propensity region. The time interval $[t^*,2t^*]$ has only four particles with propensity 36% greater than the mean value for

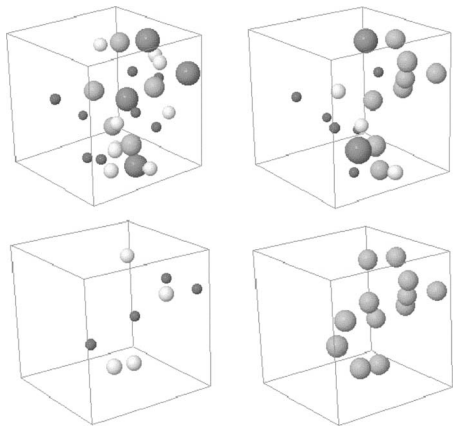

FIG. 5. Spatial distribution of high propensity particles for selected time intervals. In all cases the particles are placed at their positions at $t=0$ to better compare the different graphs. The sizes of the particles are not the real ones but increase as their propensity increases from 36–50, 75, and 100 % greater than the value of $\langle P\rangle$ for the corresponding time interval: $[0,0.1t^*]$ (top-left), $[0,t^*]$ (top-right), and $[0,4t^*]$ (bottom-left). Bottom-right: The 10% of the particles with the highest propensity for time interval $[0,10t^*]$ (in this case, the particles are drawn with their real sizes).

such time interval and only one with propensity 50% greater. None of the other time intervals presents particles with propensity 36% larger than its corresponding mean value (nor even 25% greater). All these results clearly demonstrate that the short-time fluctuations (on times of the order of 10% t^*) are able to predict the dynamical behavior at time scales of around t^*, but that they undoubtedly fail to do so for longer times on the order of the α relaxation.

The above expounded results are consistent with our previous findings that the influence of structure on dynamics is local in time [10] (at the β but not the α relaxation). In Ref. [10] we showed that the different trajectories of a given IC ensemble are at first subject to explore the same local metabasin, but that each of them escapes from it by means of a d cluster that brings them to different MBs (the MB connectivity of the potential energy surface is high, since in Ref. [10] we showed that the probability that two different trajectories go to the same second MB is lower than 1%). Thus, the MB dynamics is irreproducible, and the long time dynamics of the system can be described as a random walk on MBs. This irreproducibility of the long time dynamics is also consistent with other well established dynamical scenarios for glassy relaxation such as the dynamical facilitation model, where the dynamics at long times in 3D space cannot be predicted from the initial condition of defects [17]. With the methods of Refs. [10,16], τ_{MB} for the first MB of the IC ensemble we use in the present work is close to $t^* \approx 400$, precisely the time span over which the short time dynamics can be used to predict the spatial variation of propensity. Other IC ensembles may present a larger or lower value of τ_{MB} for the first MB (indicating that the corresponding local MB is more confining or less confining, respectively). Thus, we repeated the present study for an IC ensemble with τ_{MB} about twice ($\tau_{\mathrm{MB}} \approx 700$ also at $T=0.5$) the one we present in this work and found that for such case the short-time dynam-

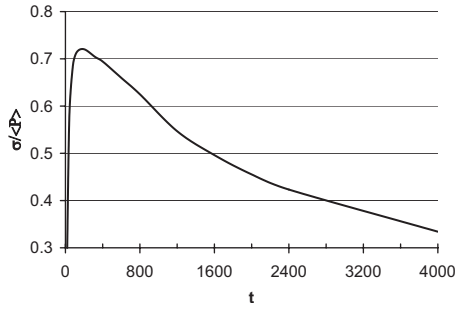

FIG. 6. $\sigma/\langle P\rangle$ of $\langle \Delta \mathbf{r}_i^2(t,10t^*)\rangle_{\mathrm{IC}}$ as a function of time.

ics could predict the dynamical behavior up to a time span of about twice the length of the one for the IC ensemble we considered here.

This point is also clear from the calculation of $\langle \Delta \mathbf{r}_i^2(t,10t^*)\rangle_{\mathrm{IC}}$ for different values of t. In Fig. 6 we show the dispersion over the mean value $(\sigma/\langle P\rangle$ for the corresponding time intervals $[t,10t^*]$). The curve at first grows, presents a maximum below and close to t^* and then decays. This is another indication that propensity is clearly heterogeneous at short times while at longer times it loses such heterogeneity. The reason for this behavior is that from times below t^* some of the 1200 trajectories of the IC are able to exit the metabasin by means of a d cluster with the concurrent relaxation of the original unjammed region and the emergence of a new unjammed one [10,16]. And since each trajectory enters a different second MB, the mobile regions after the MB transition will be different for the different trajectories.

Finally, we shall briefly comment on the relationship between the high propensity particles at short times and the particles involved in d clusters (MB transitions). In a previous work (not dealing with propensities) we showed that for this system the dynamical behavior within time spans of around t^* is almost exclusively due to the mobility in the corresponding d cluster which lasts roughly 10% such time [18] (the distribution of particle displacements averaged over many d clusters looks very similar to the van Hove function at t^*). Thus, most of the long-range movements of the particles occur at d clusters (while the rest of the time is not significantly relevant to the structural relaxation). Here we show a similar situation but we average over the IC ensemble (that is, we calculate such functions averaging over the different trajectories of an IC). In Fig. 7 we show the van Hove function for $t=10\%t^*=40$ and for $t=\tau_{\mathrm{MB}}$ (a time scale one order of magnitude larger than $10\%t^*$ [10,16]). We use here τ_{MB} since we are averaging over the IC ensemble and we want to compare the situation at short times with that at a time when most of the trajectories have left the first MB. We can see that, as expected, the van Hove function for the short-time interval is clearly displaced to the left with respect to the curve for τ_{MB}, displaying reduced mobility. In such a figure we also show the particle displacement distribution within a typical d cluster (during a $t=40$ time interval). To this end, we detected 12 different d clusters (we followed 12 different trajectories of the IC and identified the times when they abandoned the first MB, as done in previous works [9,10]). We note that these d clusters are somewhat different

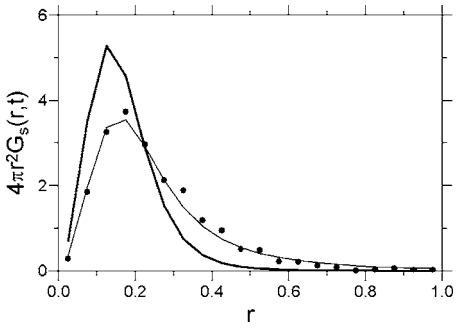

FIG. 7. The van Hove correlation function $4\pi r^2 G_s(r,t)$ for $t=40$ (thick line), $t=\tau_{\mathrm{MB}}$ (thin line), and the distribution of particle displacements for chosen d clusters (dots). The d clusters last a time scale of $t=40$.

from each other and occur at different times. We can see a great similarity between the curve for these d clusters and the van Hove function at τ_{MB}, which means that most of the dynamics in the MB exploration comes out from the d clusters. Additionally, the dynamical information in this function (which has been averaged over the IC) is similar to that of the propensity $\langle \Delta \mathbf{r}_i^2(0,\tau_{\mathrm{MB}})\rangle_{\mathrm{IC}}$ (which computes the ensemble-averaged squared displacement of the particles instead of their modulus). Thus, the similarity between the spatial distribution of propensity at short times and that at long times is an indication that the high-propensity unjammed particles are related to that involved in the exit of the MB. To emphasize this connection between short-time propensity particles and d clusters we calculated a probability to take part of the first d cluster (the one that takes the system out of the first MB for each trajectory). To this end we used the 12 d clusters above indicated and calculated for each of the 120 A particles (N) their probability to belong to a d cluster. This function, which we call d_i (where the index i runs over N), can be compared with the propensity of such A particles in a $t=40$ time span $\langle \Delta \mathbf{r}_i^2(0,40)\rangle_{\mathrm{IC}}$. We expect that many of the particles with high propensity shall show a high value of d. Figure 8 shows the cross-correlation R_i between these two functions

$$R_i = \frac{(x_i-\bar{x})(d_i-\bar{d})}{\left(\sum_i (x_i-\bar{x})^2\right)^{1/2}\left[\sum_i (d_i-\bar{d})^2\right]^{1/2}},$$

where $x_i=\langle \Delta \mathbf{r}_i^2(0,40)\rangle_{\mathrm{IC}}$, $\bar{x}=N^{-1}\Sigma_i^N x_i$, and $\bar{d}=N^{-1}\Sigma_i^N d_i$. Positive values of this correlator indicate that the two functions

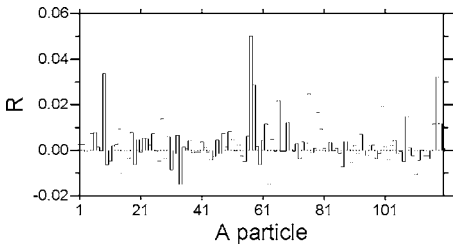

FIG. 8. Cross-correlation R between the propensity at short times $\langle \Delta \mathbf{r}_i^2(0,40)\rangle_{\mathrm{IC}}$ and the probability of the different A particles to take part in a d cluster to exit the first MB d_i.

are positively correlated while negative values indicate anticorrelation; values close to zero mean that there is no correlation between them. From direct inspection of Fig. 8 we can see that many particles show clear positive correlations between propensity at short times and probability to form a d cluster. Additionally, the sum of R_i for the 120 A particles gives a global positive correlation of 0.31.

III. CONCLUSIONS

To summarize, our results clearly demonstrate that while the very short-time dynamics (at times lower than $10\%t^*$) represents a precursor of the relaxation at times close to the metabasin lifetime (thus, being able to predict the dynamics of exploration of the local MB), the long time dynamics of the system (the MB dynamics or the α relaxation, which is completed by a small series of MB transitions [9,10]) is non predictable. In this regard, the following picture emerges for the interplay between structure and dynamics: At any given time the system posses a less jammed (high propensity) region which is dynamically more active, with enhanced particle fluctuations at short times. However, for any given trajectory, the coherent fluctuation of these particles is needed in order to undergo a structurally significant relaxation event (that is, the occurrence of a d cluster) and thus, the system remains in the given local MB for some time. All over this time the spatial distribution of dynamical propensity is implicit in the very short-time fluctuations of the system. Finally, the occurrence of a d cluster, which brings the system to a neighboring MB, relaxes the formerly unjammed region and, concurrently, a new unjammed region arises with its corresponding constraint on particle dynamics. Thus, these results constitute an indication that the dynamical scenario underlying the findings of [11] is clearly not case (1) but case (2) as described in the Introduction, in complete harmony with the picture put forth in Ref. [10] where the short-time motions can only predict dynamics at intermediate times close to the MB lifetime but not at the α-relaxation time.

ACKNOWLEDGMENTS

Financial support from ANPCyT, SeCyT, and CONICET is gratefully acknowledged.

[1] M. D. Ediger, Annu. Rev. Phys. Chem. **51**, 99 (2000).
[2] P. G. Debenedetti and F. H. Stillinger, Nature (London) **410**, 259 (2001).
[3] K. Schmidt-Rohr and H. W. Spiess, Phys. Rev. Lett. **66**, 3020 (1991).
[4] M. T. Cicerone, F. R. Blackburn, and M. D. Ediger, J. Chem. Phys. **102**, 471 (1995).
[5] C. Donati, J. F. Douglas, W. Kob, S. J. Plimpton, P. H. Poole, and S. C. Glotzer, Phys. Rev. Lett. **80**, 2338 (1998).
[6] C. A. Angell, J. Non-Cryst. Solids **131**, 13 (1991).
[7] M. Vogel, B. Doliwa, A. Heuer, and S. C. Glotzer, J. Chem. Phys. **120**, 4404 (2004).
[8] A. Widmer-Cooper, P. Harrowell, and H. Fynewever, Phys. Rev. Lett. **93**, 135701 (2004).
[9] G. A. Appignanesi, J. A. Rodriguez Fris, R. A. Montani, and W. Kob, Phys. Rev. Lett. **96**, 057801 (2006).
[10] G. A. Appignanesi, J. A. Rodriguez Fris, and M. A. Frechero, Phys. Rev. Lett. **96**, 237803 (2006).
[11] A. Widmer-Cooper and P. Harrowell, Phys. Rev. Lett. **96**, 185701 (2006).
[12] R. A. Denny, D. R. Reichman, and J. P. Bouchaud, Phys. Rev. Lett. **90**, 025503 (2003).
[13] We use reduced units as in Ref. [9].
[14] J. A. Rodriguez Fris, G. A. Appignanesi, E. L. LaNave, and F. Sciortino, Phys. Rev. E **75**, 041501 (2007).
[15] R. A. L. Vallée, M. Van der Auwerear, W. Paul, and K. Binder, Phys. Rev. Lett. **97**, 217801 (2006).
[16] M. A. Frechero, L. M. Alarcón, E. P. Schulz, and G. A. Appignanesi, Phys. Rev. E **75**, 011502 (2007).
[17] Y. J. Jung, J. P. Garrahan, and D. Chandler, Phys. Rev. E **69**, 061205 (2004).
[18] G. A. Appignanesi, M. A. Frechero, and L. M. Alarcón, Physica A **374**, 229 (2007).